INSTITUTE OF PLASMA PHYSICS

NAGOYA UNIVERSITY



ELECTROSTATIC ION CONFINEMENT

IN A MAGNETIC MIRROR FIELD

Y. Nishida*, S. Kawamata*

and

K. Ishii**

IPPJ-256 August 1976

# RESEARCH REPORT

NAGOYA, JAPAN

# ELECTROSTATIC ION CONFINEMENT IN A MAGNETIC MIRROR FIELD

Y. Nishida*, S. Kawamata*

and

K. Ishii**

IPPJ-256 August 1976

Further communication about this report is to be sent to the Research Information Center, Institute of Plasma Physics, Nagoya University, Nagoya, Japan.

---

Permanent Address :

* Electrical Engineering, Utsunomiya University, Utsunomiya, Japan.

** Institute of Plasma Physics, Nagoya University, Nagoya, Japan

## Abstract

The electrostatic ion stoppering at the mirror point is demonstrated experimentally in a magnetic mirror field. The ion losses from the mirror throat are decreased to about 15% of the initial losses in a rather high plasma density ($10^{10} < n_0 \lesssim 10^{13}$ cm$^{-3}$). It is discussed as a confinement mechanism of ions that particles are reflected back adiabatically at the throat of the magnetic mirror field supplemented by DC electric field.

## Introduction

The collisional losses from the ends of the mirror machines place substantial restrictions on the confinement time of a plasma in such an open-end device. Because of these losses it has been shown that it would be difficult to build a fusion reactor based on a mirror machine.[1] However, in recent years, various proposals have been made to utilize rf or dc electric fields to reflect escaping particles back into the system.[2-5] All of these proposals have difficulty in building a strong electric field in a plasma system. Recently two new proposals were made. One of which is that the quasi-adiabatic reflection of a plasma is achieved by the mirror magnetic field supplemented by the resonant HF field at the mirror throat.[6] The other is that the adiabatic reflection of ions is demonstrated in the magnetic mirror field supplemented by the electrostatic DC field.[7]

In this paper precise experimental results are given on the ion confinement by the electrostatic DC field superposed on the magnetic mirror field.

## Experimental Apparatus

The schematics of the experimental apparatus and the diagnostics are shown in Fig. 1. The "Region II" in Fig. 1 is the plasma producing section which is the TPD-1 machine in Nagoya University.[8] The helium plasma produced in Region II has the maximum density of the order of $10^{14}$ $cm^{-3}$, electron temperature, $T_e$, about 10 eV and ion temperature, $T_i$, 10 ~ 20 eV in steady state, and diffuses into the plasma trapping section, "RegionI", through orifices $0_0$, $0_3$ and $0_1$ . The orifice $0_0$ with a hole of 2.5 cm in diameter is the floating water-cooled electrode. Orifices $0_3$ and $0_4$ with a

hole of 2.0 cm in diameter are made of ceramics. Orifices $O_0$ and $O_3$ are settled to protect the direct coupling between the plasma source and the plasma trapping section, although the decoupling is not complete in the present stage. Orifices $O_1$ and $O_2$ with a hole of 3.0 cm in diameter are made of a conductor and can be biased up to 500 V against the anode electrode, A, which is grounded. The plasma trapping section is surrounded by an annular electrode with a diameter of 15 cm by the length of 50 cm, named H-electrode in Fig. 1. The maximum magnetic field strength at the throat is 5.9 kG and the maximum mirror ratio, R, is 2.0.

An electron temperature and its radial profile, a plasma density profile and the instabilities occurring in the plasma are measured by the Langmuir Probe, $P_1$. The plasma space potential is measured by an emissive probe,[9] settled in a center of the magnetic mirror configuration. The ion losses from the mirror point is measured by a probe, $P_2$, which is in the off-axis about 3 ~ 5 mm, and is biased fully negative. An ion temperature is determined from a full-half width of the Doppler broadening of HeII (4686 Å) line, by using a double-monochromator. The ion temperature thus obtained is the perpendicular component to the magnetic field.

## Experimental Results

The plasma in the trapping section has initially a diameter of about 2 cm in the center of the mirror field and the density which is varied between $10^{10}$ to several times $10^{13}$ $cm^{-3}$ by the change of the discharge currents of the plasma source up to 100 A in the neutral pressure of $(0.5 \sim 1.0) \times 10^{-3}$ Torr.

To test the independence of the heating section from the plasma source we applied the positive DC voltage on the electrode H and orifices $O_1$ and $O_2$ against the ground. We cannot observe the clear change in the plasma source region in the course of our experiment so we may say that the results, which will be given later, are the phenomena mainly occurring in Region I.

The typical examples of the plasma losses from the mirror throat and the change of the plasma profiles are shown in Figs. 2 and 3 as a function of the applied DC voltage.

In Fig. 2, $O_1$, $O_2$ and H are in the same potential, i.e. they are connected electrically, and in Fig. 3, $O_1$ and $O_2$ are at the floating potential and the high voltage is applied only on the H-electrode. The plasma loss rate is estimated as $\delta = I_i(V_H)/I_i(V_H = 0)$ which is the function of the applied voltage $V_H$, where $I_i$ is the ion saturation current of the probe $P_2$. The plasma losses are decreased to roughly $\delta = 50\%$, this rate does not depend on the probe bias. If $V_H$ becomes larger than about 300 V, the discharge occurs within the trapping section and so the plasma production occurs. This is because the neutral pressure in region I is not low enough. Therefore, we are interested in the region where $V_H$ is smaller than about 300 V. The corresponding change of the plasma profile in the radial direction is shown in Fig. 2-b. As is clearly seen in Fig. 2-b, the ion saturation current around the column center decreases as the applied voltage, $V_H$, increases, while ion currents around $r \simeq 1.2$ cm increase. This means that the ions are trapped between electrodes $O_1$ and $O_2$, and that the plasma is the annular type. In other words, the decrease of loss rate $\delta$ is dependent on the fact

that the plasmas are blown off from the center region toward the outside (this mechanism will be discussed later) and so the plasma density decreases on the axis, while in the off-axis region the plasma density increases if the ions are trapped between electrode $O_1$ and $O_2$. The same kind of data are shown in Fig. 3 with a different electrode connection from Fig. 2. In this case we can apply a much higher voltage on H than in the case of Fig. 2 and the ion losses from the mirror throat are decreased about 70% or more of the initial loss as shown in Fig. 3. The floating potentials of the electrodes $O_1$ and $O_2$ shown in the same figure, increase rapidly as the ion losses from the mirror throat decrease. The floating potential of these electrodes are determined by the relation of the electron temperature and the ion temperature but we can say that a part of the ions is retarded and reflected back if its kinetic energy is smaller than the potential energy of the electrodes. The plasma profiles corresponding to Fig. 3 are shown in Fig. 4. As is clearly seen the ion current in the center of the column decreases as the $V_H$ increases while the ion current in the peripheral region increases, as is a similar manner to that shown in Fig. 2. The plasma boundary (the wall of the electrode H) in this case is at 7.3 cm. The variation of the plasma floating potential corresponding to Figs. 3 and 4 is shown in Fig. 5. We actually need a plasma space potential but we cannot measure it because the probes melt away with high plasma density and high ion temperature. The floating potential is different from the real plasma space potential even though we may say that the electric field strength in the radial direction $E_r$ increases as the $V_H$ increases. It is easily suspected that ions are reflected back if the perpendicular kinetic energy

of ions (= $M V_{\perp}^2/2$, where M is the mass of ion and $V_{\perp}$ is the perpendicular velocity component of the ion) is smaller than the electrode potential ($\leq eV_H$). Even if the discharge currents and so the plasma densities, are increased more, the rate of decrease of ion loss essentially does not change as shown in Fig. 6. In these higher current cases we unfortunately cannot measure even the plasma floating potential as the water cooled probe cannot be used anymore. When there is no electrode such as orifices $O_1$ and $O_2$, we cannot observe the phenomena such that the ion loss rate decreases or that the ion current increases in the intermediate region between the column axis and the wall electrode H even if $V_H$ becomes high enough. These facts mean that the electrodes $O_1$ and $O_2$ are effective for ion confinement in a mirror field.

When the diameter of the plasma source is increased from 8 mm, which is used so far, to 15 mm but those of the orifices are kept constant, the plasma density decreases if other discharge conditions are kept constant. The plasma space potential and the profiles can be measured in such a slightly different plasma condition. The typical example is shown in Fig. 7 in which the orifices $O_1$ and $O_2$ are at the floating potential. The plasma profiles measured from ion saturation currents are shown in Fig. 7-a. The plasma concentrates in a center region in a rather low voltage of $V_H$, but the $V_H$ becomes large enough the plasma diffuses toward the outside and finally the outside density becomes larger than that of the center. In the outermost region on the other hand, the plasma density decreases again, which corresponds to the fact that the potential of the electrode $V_H$ is high enough and that as a result the ions are retarded back into the center region. Consequently, a thin sheath-like region exists in front of the electrode H. This phenomenon is also confirmed by the space potential measurement. The

space potentials shown in Fig. 7-b are measured by the emissive probe under the conditions corresponding to Fig. 7-a. As is clearly seen from these results the radial electric field strength increases as the applied $V_H$ increases and the two strong electric field regions exist near a column axis and just in front of the electrode $V_H$. When the discharge current becomes larger than about 30 A, which is finally varied up to 50 A, we cannot measure the plasma profile and the space potential within Region I because the water cooled orifices $O_0$ and $O_3$ in the present case vaporized with a high plasma density and the metalic impurities came into the plasma. Roughly speaking, however, the same phenomena occurring in a small discharge current condition might be expected in the large discharge current condition because the throat losses of the ions are decreased almost at the same rate as in the case of the small discharge current.

Discussion

The profile of the plasma space potential may be divided into two typical regions. One is the negative potential region and the other is the positive potential region against the ground potential (see Fig. 5 or 7-b). The negative potential region is essentially determined by the plasma source conditions and we cannot control it if the plasma source conditions are fixed. The relatively low energy ions are trapped in this negative potential region. The potential profiles of the outer positive potential region on the other hand, are controlled by changing the applied voltage $V_H$. The ions with rather higher kinetic energy which are not trapped by the inner potential well, are retarded in this outer potential well. Thus ions existing in the outer positive potential region have generally a larger kinetic energy than the ions existing in the negative potential regions.

The trapping conditions of the ions in a mirror machine with a static electric field may be given as following in our case,

$$v_{\parallel}^2 < 2\,eV_o/M + v_{\perp}^2\,(R-1) \qquad (1)$$

at the mirror point and

$$v_{\perp}^2 < 2\,eV_H/M \qquad (2)$$

at the surface of the electrode H, where $v_{\parallel}$ and $v_{\perp}$ are the parallel and perpendicular component of the velocities at the center of the machine, respectively, $V_o$ and $V_H$ are the potential of the orifices $O_1$ or $O_2$ and the electrode H, respectively, R is the mirror ratio and M is the ion mass. These conditions are satisfied if the adiabatic condition of ions is satisfied. If $V_o = 0$, Eq. (1) shows the familiar adiabatic reflection condition in the mirror field. When, on the other hand, the static potential is strong enough, i.e. $eV_o > MV_{\perp}^2(R-1)/2$ is satisfied, even the particles which are scattered into the loss cone are reflected back, i.e. the effective loss cone becomes small. The adiabatic condition is not necessarily satisfied fully in the whole volume of the present experimental apparatus, rather than the plasma is non-adiabatic in the present experiment. But the adiabatic condition, as it were, the local adiabatic condition, could be satisfied near the mirror throat where there is no ion heating, and this might be enough for ion reflection at the mirror throat.

The electrostatic field is built as already shown experimentally through the electron currents flowing into the electrode $O_1$, $O_2$ and H across the magnetic field lines, when $V_o$ and $V_H$ are applied. The machine

is designed so that the direct electron currents from the source along the magnetic field lines are suppressed as small as possible by using the insulated orifices $O_0$ and $O_3$. This is essential for building the strong radial electric field confining the ions with the electrostatic potential well in a mirror machine. The ion flux $I_i(V_H)$ measured by the probe $P_2$ might not necessarily be the ion loss flux. The rigorous ion loss rate should be defined as the ratio of $I_i$ (output)/$I_i$ (input), where $I_i$ (output) and $I_i$ (input) are the ion flux from and into the mirror field, respectively. If $I_i$ (input) is kept constant, $\delta$ corresponds to the ion loss rate from the mirror throat. Actually, however, the input throat of the mirror field is also choked by the condition given by Eq. (1), and the decrease of $\delta$ contains the components of the decrease of plasma input from the source. The plasma losses within the potential well in a mirror field could never be zero, as the charge exchange losses and others will exist. So, the electric field $V_H$ should be preferred to be AC field with a frequency much lower than the inverse of the characteristic loss time. This type of experiment is now undertaken.

When the voltage $V_H$ is applied, the strong radial electric field is formed. This field causes the plasma body rotation and some instabilities, especially $E_r \times B$ type or lower hybrid waves,[10] resulting in strong ion heating. Actually we have measured the ion temperature up to 300 ~ 400 eV in steady state, but the precise results on these phenomena are out of the present scope and will be reported in a separate paper. We can say that the $E \times B$ type plasma rotation is important for the plasma confinement, because the ions are blown away from the center region toward the outside, escaping from the loss cone of the mirror field supplemented by DC electric field.

Summary

In this paper the possibilities of ion confinement by the electrostatic potential well have been shown experimentally in a plasma with rather high density in a magnetic mirror field. The ion losses from the mirror point have been decreased to be about 15% of the initial losses. Some discussions on the ion confinement and the confinement conditions are given.

Acknowledgements

The authors are grateful to Prof. K. Takayama for his continuous encouragements. This work was performed under the Collaborating Research Program of the Institute of Plasma Physics, Nagoya University.

References

1. D.V. Sivukin, Plasma Phys. 8, 607 (1966).
2. A.A. Ware and J.E. Faulkner, Nucl. Fusion 9, 343 (1969).
3. C.J.H. Watson and L.G. Kuo-Petravic, Phys. Rev. Lett. 27, 1231 (1968).
4. R.W. Moir, W.I. Barr, and R.F. Post, Phys. Fluids 14, 2531 (1971).
5. B.B. McHarg Jr., and N.E. Oakes, Phys. Fluids 17, 1923 (1974).
6. V.D. Dougar-Jabon, K.S. Golovaninsky, and V.I. Karyaka, in Proceedings of Seventh European Conference on Controlled Fusion and Plasma Physics, proceedings (Lausanne, 1975), vol. 1, p. 33.
7. Y. Nishida, S. Kawamata, and K. Ishii, in Proceedings of Seventh European Conference on Controlled Fusion and Plasma Physics, proceedings (Lausanne, 1975), vol. 1, p. 34.

8. K. Takayama, M. Otsuka, Y. Tanaka, K. Ishii, and Y. Kubota, in Proceedings of the Eighth International Conference on Phenomena in Ionized Gases, Vienna, 1967 (Springer, Berlin, 1967), p. 551.

9. R.F. Kemp, and J.M. Sellen, Jr., Rev. Sci. Instr. 37, 455 (1966).

10. A. Hirose and I. Alexeff, Nucl. Fusion 12, 315 (1972).

Figure Captions

Fig. 1 Experimental arrangement and the magnetic field configuration

Fig. 2 (a) Ion loss rate vs the applied confinement voltage $V_H$. Insert shows the electrode connection. (b) Ion saturation current $I_{si}$ vs the radial position as a parameter of $V_H$. Discharge current $I_d$ = 4A, $B_{max}$ = 4.6 kG and P = $6.5 \times 10^{-4}$ Torr.

Fig. 3 Ion loss rate and the floating potentials of $O_1$ and $O_2$ vs the applied confinement voltage $V_H$. Insert shows the electrode connection $I_d$ = 5A, $B_{max}$ = 4.6 kG and P = $9 \times 10^{-4}$ Torr.

Fig. 4 Ion saturation current $I_{si}$ vs the radial position as a parameter of $V_H$ corresponding to Fig. 3.

Fig. 5 The variation of plasma floating potential in radial direction as a parameter of $V_H$. $I_d$ = 5A, $B_{max}$ = 4.6 kG and P = $9 \times 10^{-4}$ Torr.

Fig. 6 Ion loss rate vs the applied confinement voltage $V_H$ in rather high discharge current (high density) cases.
——— : $I_d$ = 10A, ——— ¯ ———: $I_d$ = 20A, ····: $I_d$ = 30A and
——— -- ———: $I_d$ = 50A. $B_{max}$ = 4.6 kG and P ≃ $(0.7 \sim 1.0) \times 10^{-3}$ Torr.

Fig. 7 (a) Ion saturation current $I_{si}$ vs the radial direction. Insert shows the electrode connection. (b) Plasma space potential vs the radial position, measured by the emissive probe.
$I_d$ = 10A, $B_{max}$ = 4.0 kG and P = $5.6 \times 10^{-4}$ Torr.

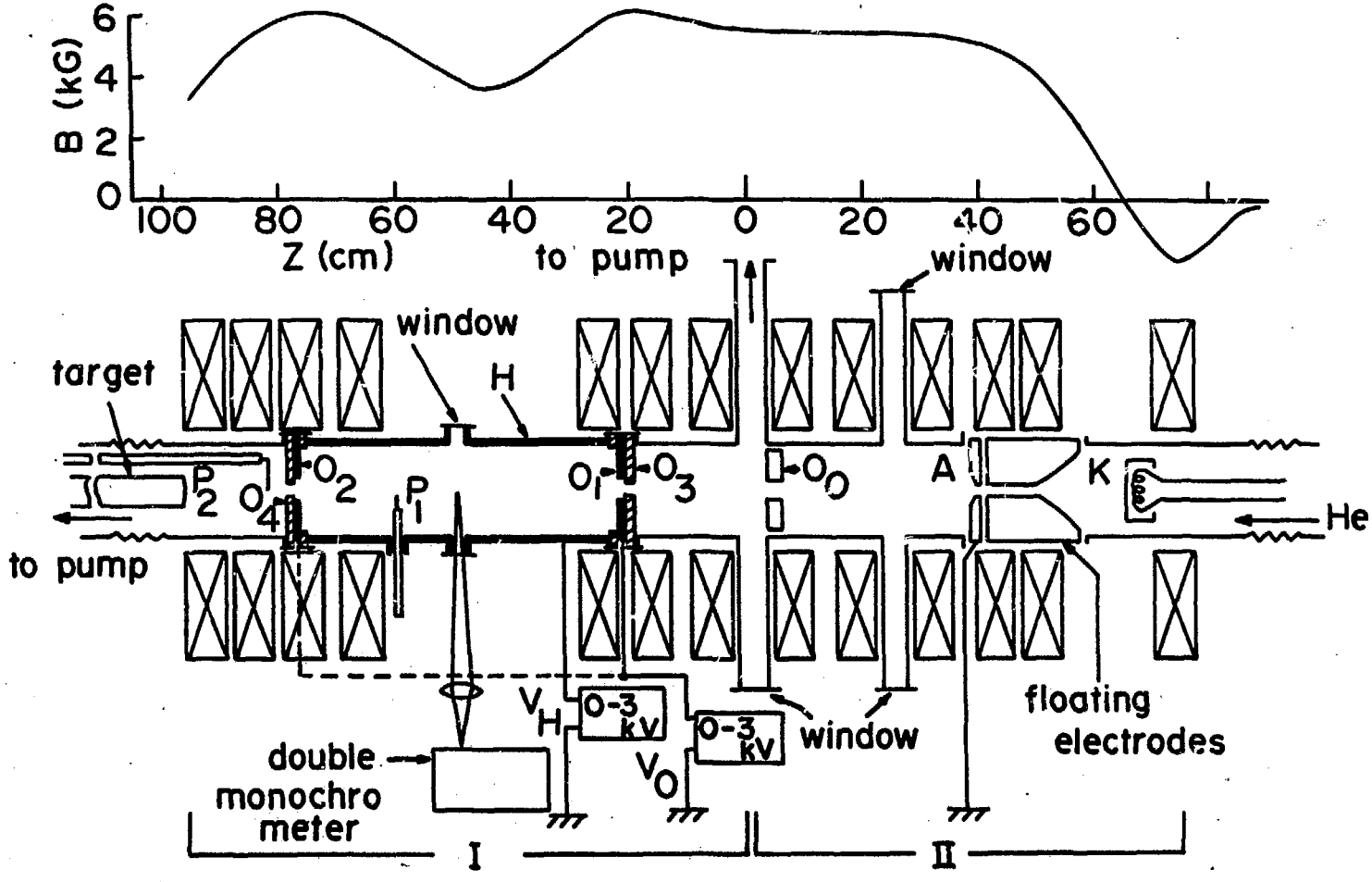
B (kG)
6
4
2
0
100
80
60
40
20
0
20
40
60
Z (cm)
to pump
window
target
window
H
$O_2$
$O_1$
$O_3$
$O_0$
$O_4$
$P_2$
$P_1$
A
K
He
to pump
$V_H$
0-3 kv
0-3 kv
$V_O$
window
floating electrodes
double monochro meter
I
II

Fig. 1

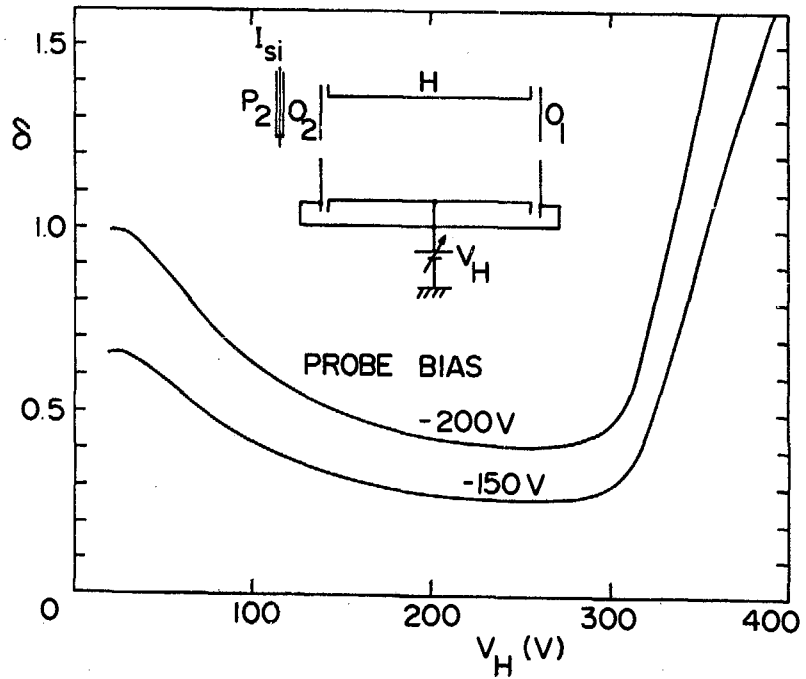
1.5
1.0
0.5
0
δ
$I_{si}$
$P_2$
$O_2$
H
$O_1$
$V_H$
PROBE BIAS
-200V
-150V
100
200
300
400
$V_H$ (V)

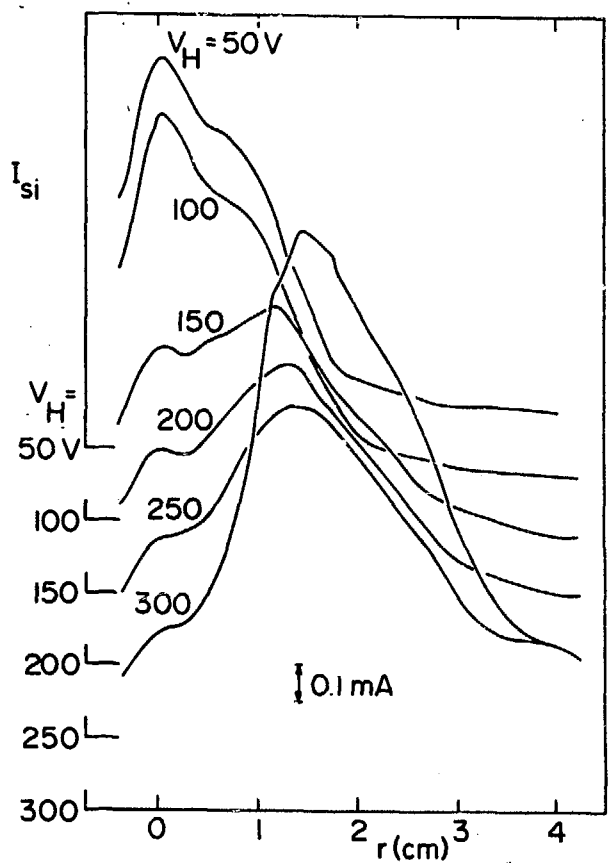
$V_H$ = 50 V
$I_{si}$
100
150
200
250
300
$V_H$ =
50 V
100
150
200
250
300
0.1 mA
0
1
2
3
4
r (cm)

Fig. 2

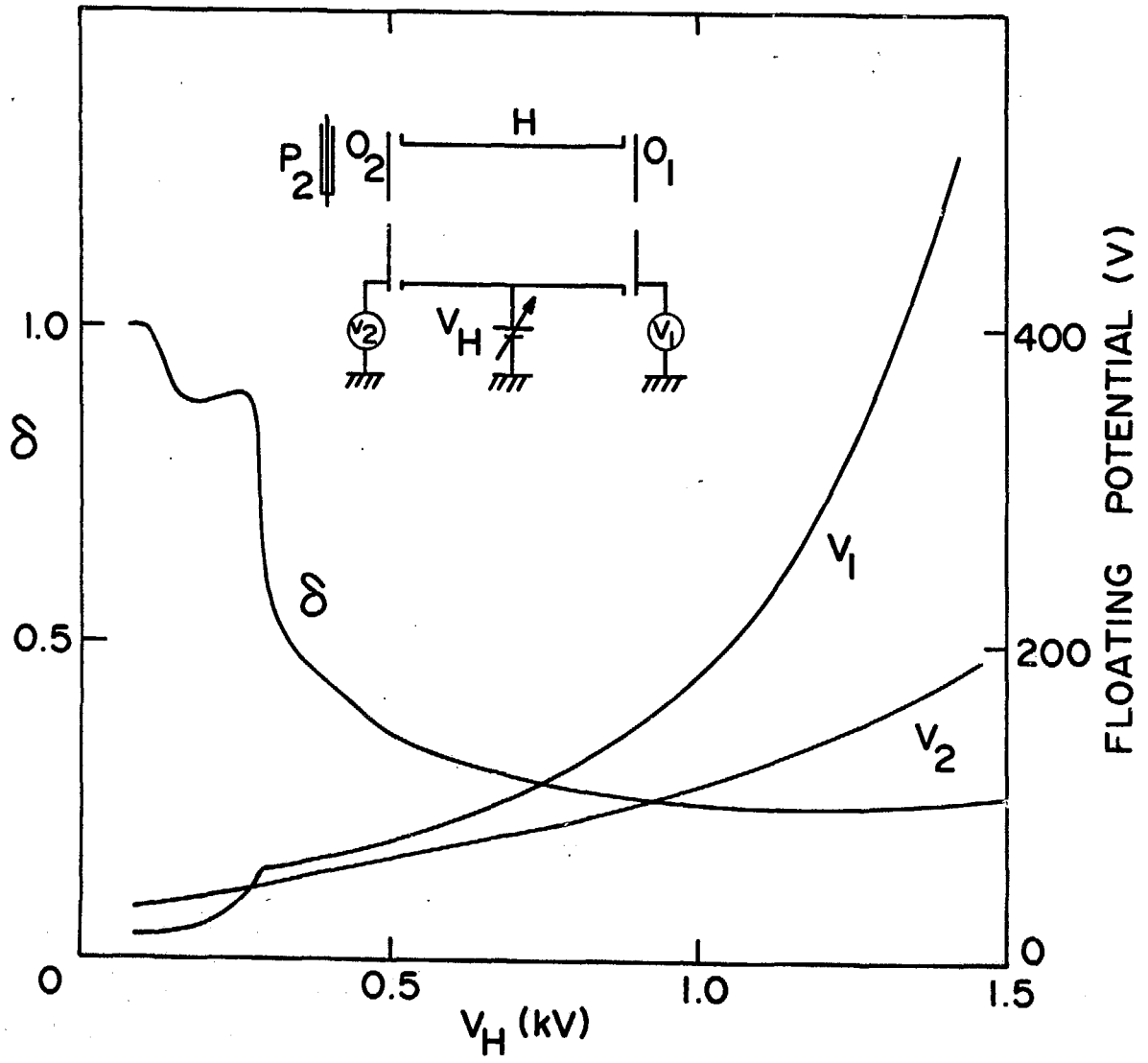
H
P2
O2
O1
V2
VH
V1
1.0
0.5
0
δ
δ
V1
V2
400
200
0
FLOATING POTENTIAL (V)
0.5
1.0
1.5
VH (kV)

Fig. 3

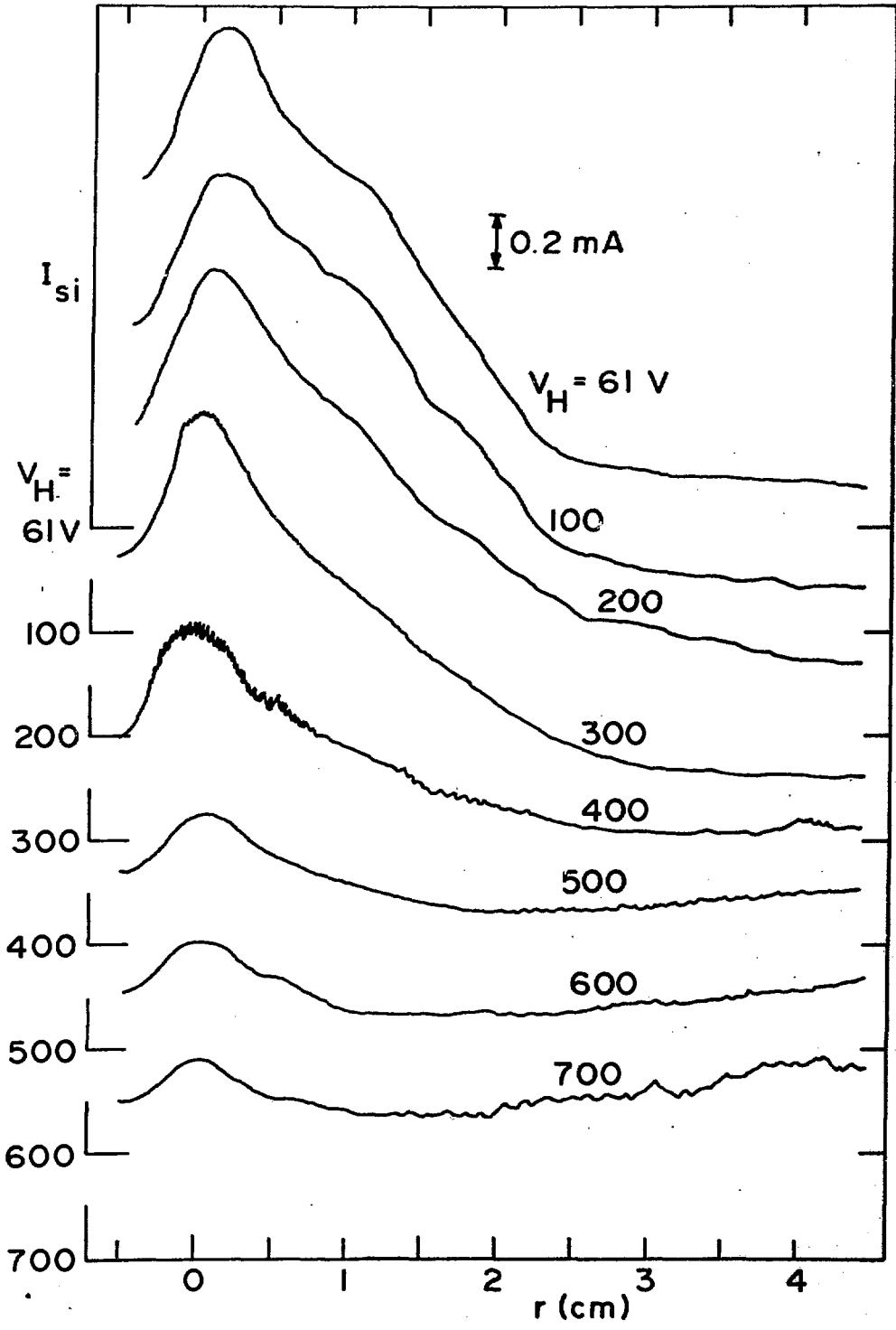


Fig. 4

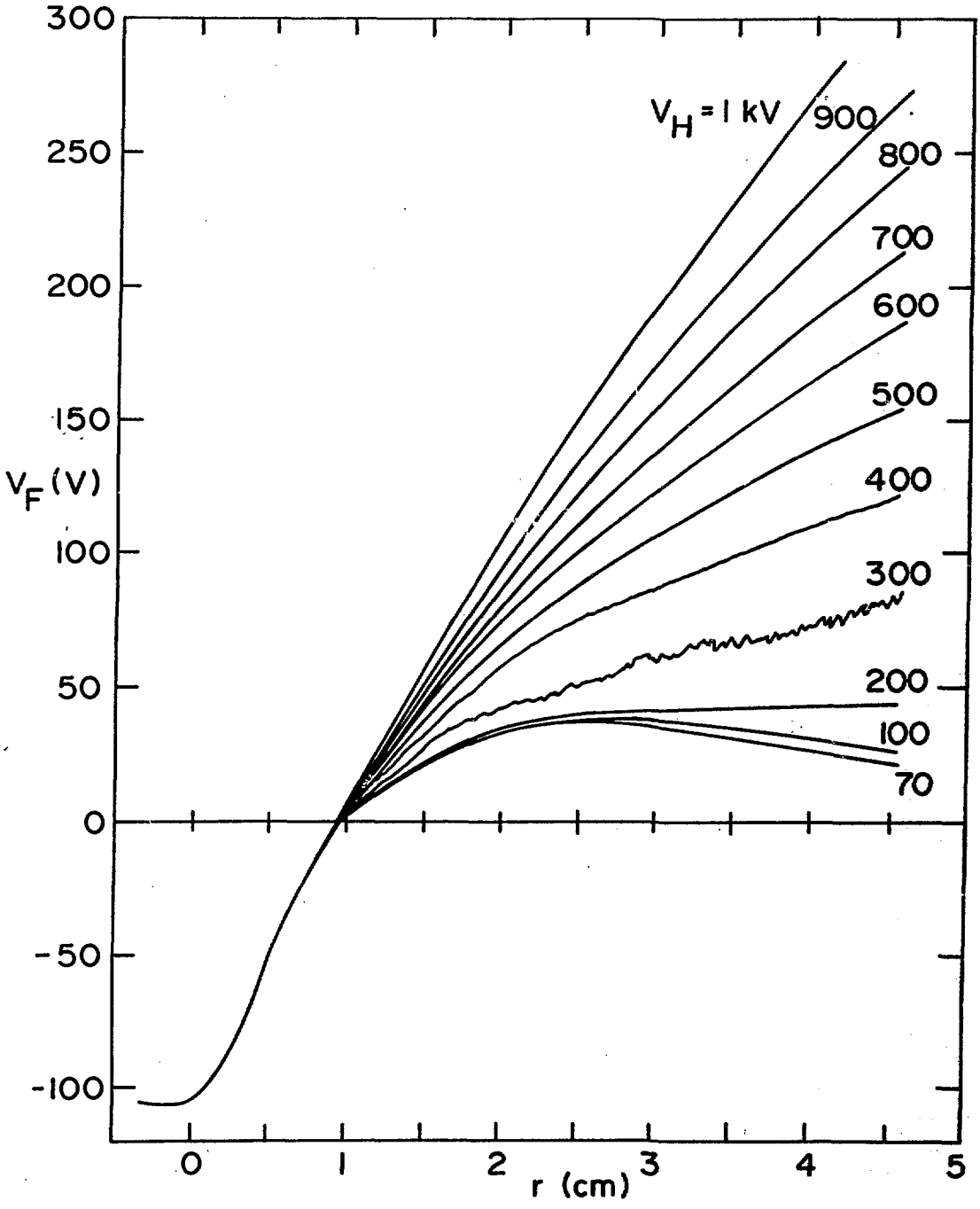
300
250
200
150
100
50
0
-50
-100
$V_F$ (V)
$V_H$ = 1 kV
900
800
700
600
500
400
300
200
100
70
0
1
2
3
4
5
r (cm)

Fig. 5

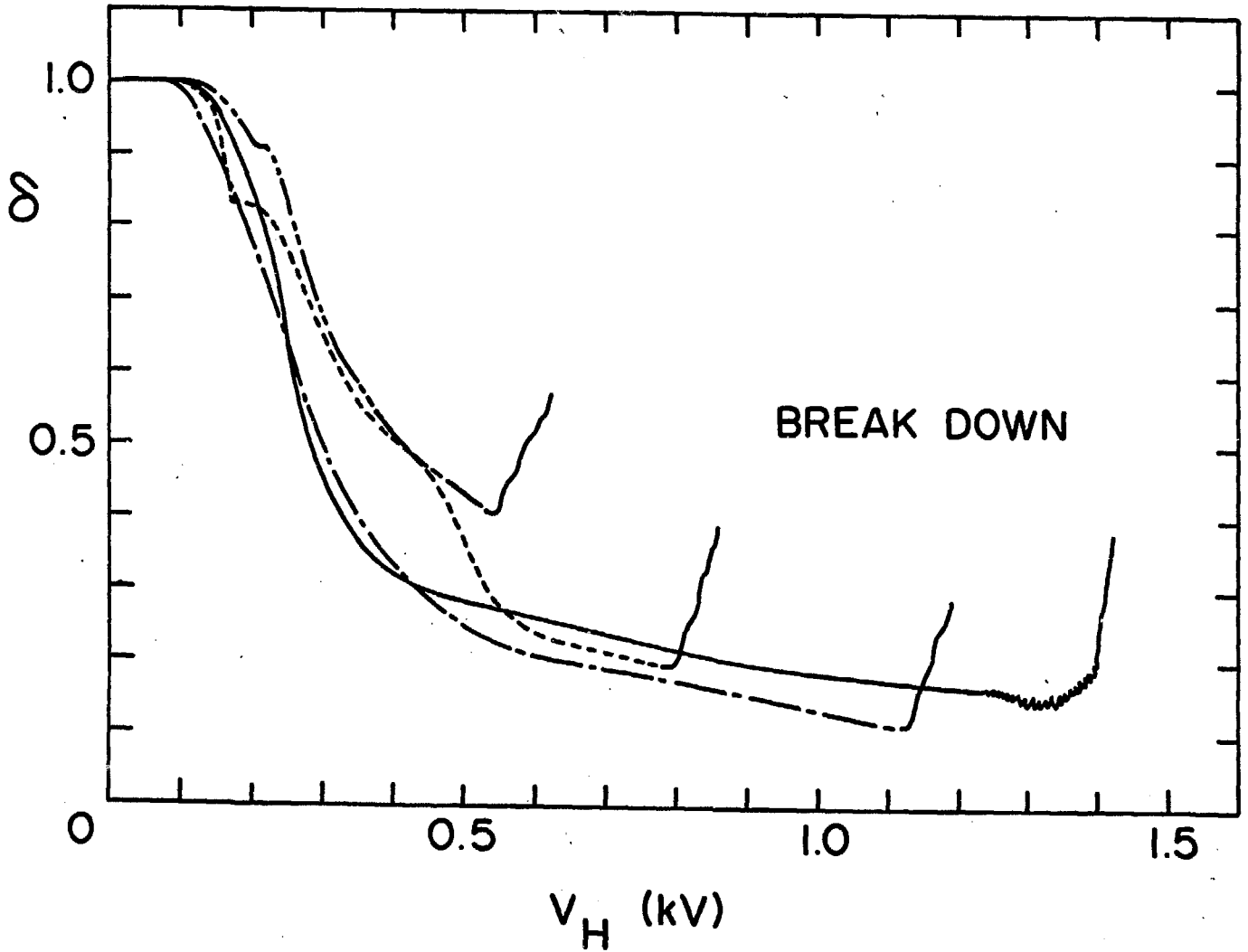


Fig. 6

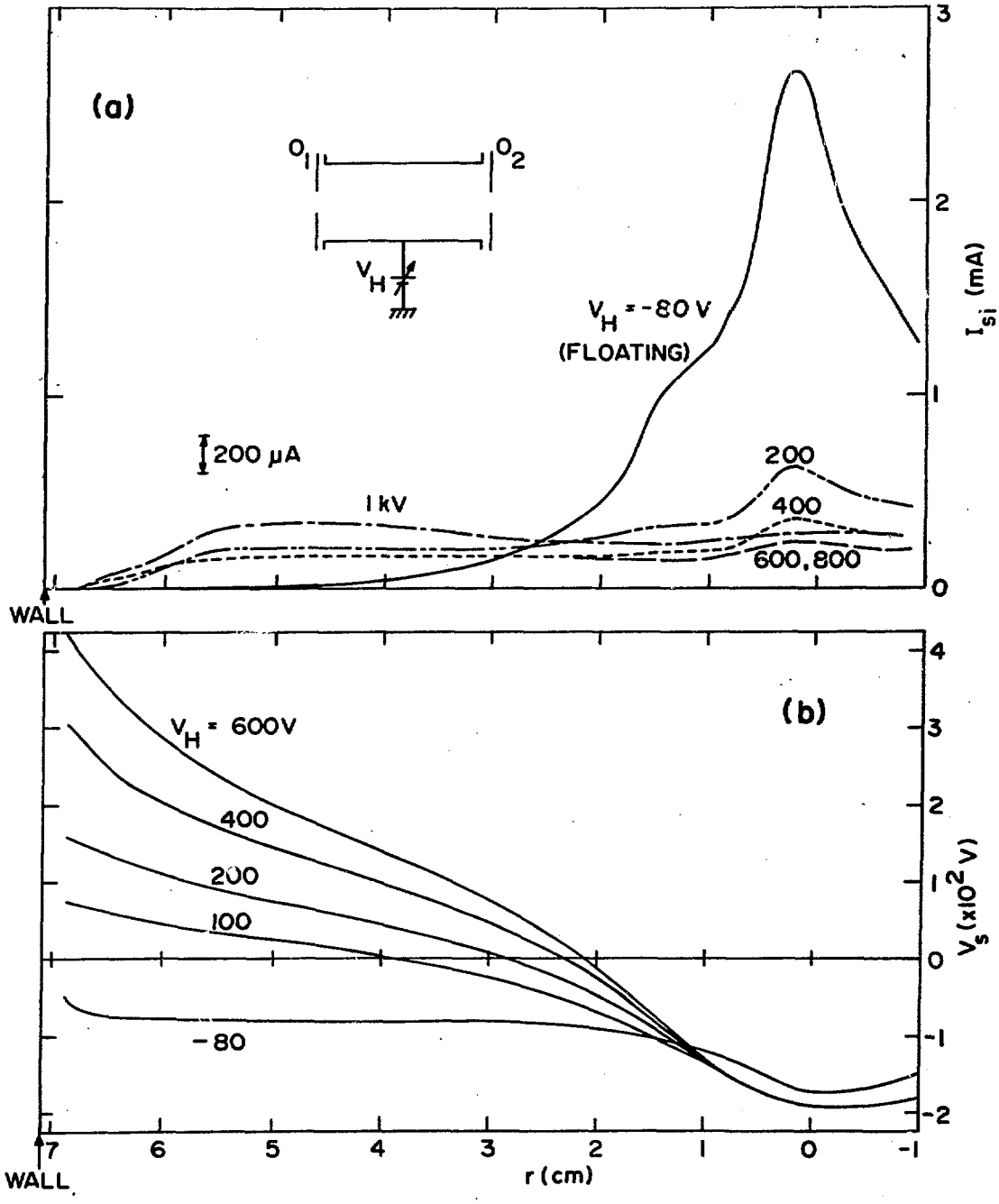
(a)
$O_1$
$O_2$
$V_H$
$V_H$ = -80 V
(FLOATING)
200 μA
1 kV
200
400
600, 800
WALL
$I_{si}$ (mA)
3
2
1
0
(b)
$V_H$ = 600V
400
200
100
-80
WALL
7
6
5
4
3
2
1
0
-1
r (cm)
$V_s$ (x10$^2$ V)
4
3
2
1
0
-1
-2

Fig. 7